

Pseudo-scalar Higgs production at next-to-leading order SUSY-QCD

Robert V. Harlander and Franziska Hofmann

Institut für Theoretische Teilchenphysik, Universität Karlsruhe

D-76128 Karlsruhe, Germany

E-mail: robert.harlander@cern.ch, fhofmann@particle.uni-karlsruhe.de

ABSTRACT: The production rate of the CP-odd Higgs boson in the Minimal Supersymmetric Standard Model is evaluated through next-to-leading order in the strong coupling constant. The divergent integrals are regulated using Dimensional Reduction, with a straightforward implementation of γ_5 . The result is confirmed within Dimensional Regularization where γ_5 is implemented according to the Standard Model calculation of Chetyrkin *et al.* [16]. The well-known Standard Model result is recovered if the masses of the supersymmetric particles tend to infinity.

KEYWORDS: Higgs production, hadron collider, supersymmetry, next-to-leading order calculations.

Contents

1. Introduction	1
2. Notation and Leading Order Result	3
2.1 Lagrangian	3
2.2 Hadronic cross section	4
2.3 Standard Model limit and leading order result	4
3. Higher orders	5
3.1 Standard Model result – Effective Lagrangian	5
3.2 SUSY contributions	6
4. Results	8
5. Discussion	10
5.1 Coefficient function \tilde{C}_1	10
5.2 Effects on the cross section	12
6. Conclusions	14

1. Introduction

The Minimal Supersymmetric Standard Model (MSSM) predicts a fundamental CP-odd scalar particle A , commonly referred to as the pseudo-scalar Higgs boson. One of the most important properties that distinguishes it from its CP-even analogues h and H is the absence of tree-level couplings to the electro-weak gauge bosons W and Z . Decay and production processes through these particles, which have been shown to be extremely helpful for CP-even Higgs searches and studies, are thus very much suppressed. This leaves associated $t\bar{t}A$ and $b\bar{b}A$ production as well as the loop-induced gluon fusion process as the most important production modes of a pseudo-scalar Higgs boson at the Large Hadron Collider (LHC) (for a recent review, see Ref. [1]). In this paper, we present the evaluation

of the inclusive gluon fusion cross section through next-to-leading order (NLO) in the strong coupling constant.

Despite the fact that the tree-level $gg\phi$ coupling vanishes ($\phi \in \{h, H, A\}$), gluon fusion in general has a comparatively large cross section because of the high gluon luminosity at the LHC, and the large top-Yukawa coupling. In the limit where squarks and gluinos are decoupled, QCD corrections have been evaluated through NNLO [2–6] by employing an effective Lagrangian for heavy top quarks (cf. Sect. 3.1); they have been shown to be numerically significant but perturbatively well-behaved.

A precise determination of the gluon fusion cross section at the LHC could yield sensitivity to as yet undiscovered particles that may mediate the $gg\phi$ coupling apart from the top and bottom quarks. Within the MSSM, for example, top squarks can play a significant role if they are lighter than around 400 GeV (recall that the Yukawa coupling for squarks is typically proportional to m_q^2 rather than m_q). In the case of CP-even Higgs bosons, such effects occur already at leading order (LO) (i.e., 1-loop). The NLO result was obtained in Ref. [7] within an effective theory for top, stop, and gluino masses much larger than the Higgs mass.

For the CP-odd Higgs boson, however, squarks do not affect the ggA vertex at 1-loop level due to the structure of the $A\tilde{q}\tilde{q}$ coupling, as will be shown below. The two-loop effects are thus expected to have a larger influence than for the CP-even Higgs production. What adds to this is that, in the limit of large m_q , the quark mediated contribution to the ggA vertex does not receive any QCD corrections owing to the Adler-Bardeen theorem. As we will show, the only 2-loop QCD effects to this coupling are due to mixed gluino-quark-squark diagrams in this limit, leading to a potentially increased sensitivity to the gluino mass. Of course, the heavy quark limit is not applicable for the bottom mediated gluon-Higgs coupling which does receive QCD corrections [8–10].

The calculation involves a technical issue that deserves special mention, namely the implementation of γ_5 within Dimensional Reduction (DRED). Its mathematically consistent and practically feasible formulation has been a subject of interest for many years now [11] (for recent developments concerning DRED, see Ref. [12,13]). Here we adopt an approach close to the prescription of Refs. [14,15]. In addition, we perform the calculation using Dimensional Regularization (DREG) with γ_5 implemented as in Ref. [16] and find full agreement with the result obtained in DRED.

Another important consistency check for our calculation is obtained from the SM limit: even for an infinitely heavy supersymmetric (SUSY) spectrum, the SUSY diagrams give a non-vanishing contribution which exactly cancels the top mass counter-term contribution arising from the LO SM diagram. The well-known result of vanishing higher order corrections to the quark-mediated ggA coupling, as required by the Adler-Bardeen theorem, is thus recovered in a non-trivial way. Combining this observation with the considerations of Ref. [13], it seems possible that in a supersymmetric theory the formal difficulties of DRED do not pose serious technical problems in practical calculations.

The outline of this paper is as follows: In Sect. 2 we introduce our notation and quote the LO result for the partonic process $gg \rightarrow A$. In Sect. 3, the effective Lagrangian underlying our calculation is introduced and the treatment of γ_5 is discussed. Sect. 4 outlines the method of the calculation and discusses the general structure of the result. It also provides analytic formulae in some limiting cases. The numerical influence of the NLO terms is discussed in Sect. 5. In Sect. 6 our findings are summarized and an outlook on possible extensions of this work is given.

2. Notation and Leading Order Result

2.1 Lagrangian

We write the underlying Lagrangian in the following form:

$$\mathcal{L} = \mathcal{L}_{\text{QCD}} + \mathcal{L}_{qA} + \mathcal{L}_{\text{SQCD}} + \mathcal{L}_{\tilde{q}A}, \quad (2.1)$$

where

$$\mathcal{L}_{qA} = i \sum_q \frac{m_q}{v} g_q^A \bar{q} \gamma_5 q A, \quad \mathcal{L}_{\tilde{q}A} = \sum_q \sum_{i=1}^2 \frac{m_q^2}{v} \tilde{g}_{q,ij}^A \tilde{q}_i \tilde{q}_j A. \quad (2.2)$$

The sums \sum_q run over all quark flavors. m_q is the mass of the quark q and $v \approx 246$ GeV the Higgs vacuum expectation value; the coupling constants g_q^A and $\tilde{g}_{q,ij}^A$ will be defined below. \mathcal{L}_{QCD} denotes the full QCD Lagrangian with six quark flavors, while $\mathcal{L}_{\text{QCD}} + \mathcal{L}_{\text{SQCD}}$ is the supersymmetric extension of \mathcal{L}_{QCD} within the MSSM, i.e., $\mathcal{L}_{\text{SQCD}}$ incorporates kinetic, mass, mixing, and interaction terms of all the squarks and gluinos. Since we will be concerned with higher orders in the strong coupling α_s only, A does not appear as a dynamical field and does not require a kinetic or a mass term.

\tilde{q}_1, \tilde{q}_2 denote the squark mass eigenstates which are related to the chiral eigenstates \tilde{q}_L, \tilde{q}_R (the superpartners of the left- and the right-handed quark q) through

$$\begin{pmatrix} \tilde{q}_1 \\ \tilde{q}_2 \end{pmatrix} = \begin{pmatrix} \cos \theta_q & \sin \theta_q \\ -\sin \theta_q & \cos \theta_q \end{pmatrix} \begin{pmatrix} \tilde{q}_L \\ \tilde{q}_R \end{pmatrix}. \quad (2.3)$$

The coupling constants relevant for the following discussion are¹

$$\begin{aligned} g_b^A &= \tan \beta, & g_t^A &= \cot \beta, & \tilde{g}_{t,11}^A &= \tilde{g}_{t,22}^A = 0, \\ \tilde{g}_{t,12}^A &= -\tilde{g}_{t,21}^A = \frac{m_{\tilde{t}_1}^2 - m_{\tilde{t}_2}^2}{2m_t^2} \sin 2\theta_t \cot \beta + \frac{\mu^{\text{SUSY}}}{m_t} (\cot^2 \beta + 1). \end{aligned} \quad (2.4)$$

The effect of quarks other than bottom and top can be neglected because of their small Yukawa couplings. Bottom and sbottom effects are typically of order $(m_b^2/M_A^2) \tan^2 \beta$

¹For a more complete collection of Feynman rules, see Ref. [17], for example.

relative to the top and stop effects. In this first analysis of NLO squark effects to pseudo-scalar Higgs production, we neglect the effect of sbottom quarks; they require a further extension of our approach. Our results are thus strictly valid only for not-too-large values of $\tan\beta$. Pure bottom effects, on the other hand, will be included through NLO in our numerical analysis.

2.2 Hadronic cross section

The cross section for the hadronic process $pp \rightarrow A + X$ at a center-of-mass energy \sqrt{s} is determined by the formula²

$$\sigma(z) = \sum_{i,j \in \{q, \bar{q}, g\}} \int_z^1 dx_1 \int_{z/x_1}^1 dx_2 \varphi_i(x_1) \varphi_j(x_2) \hat{\sigma}_{ij} \left(\frac{z}{x_1 x_2} \right), \quad z := \frac{M_A^2}{s}, \quad (2.5)$$

where $\varphi_i(x)$ is the density of parton i inside the proton. $\hat{\sigma}_{ij}$ is the cross section for the process $ij \rightarrow A + X$, where, as indicated in Eq. (2.5), i and j are parton labels. For our numerical analysis, we will use the MRST parton density sets throughout this paper [18, 19].

Sample diagrams for $ij = gg, gq, q\bar{q}$ that contribute to the inclusive Higgs production rate at LO and NLO are shown in Fig. 1.

2.3 Standard Model limit and leading order result

In the limit where all SUSY masses tend to infinity (denoted in the following by $M_{\text{SUSY}} \rightarrow \infty$), the Lagrangian of Eq. (2.1) reduces to

$$\mathcal{L}^{\text{SM}} = \mathcal{L}_{\text{QCD}} + \mathcal{L}_{qA}. \quad (2.6)$$

This will be called the ‘‘Standard Model (SM)’’ limit in what follows, despite the fact that the SM does not contain a CP-odd Higgs boson. Consequently, diagrams without any squark and gluino lines will be called ‘‘SM diagrams’’ (e.g. Fig. 1 (a)–(f)), while ‘‘SUSY diagrams’’ contain at least one propagator of a SUSY particle (Fig. 1 (g)–(j)).

Note that due to the antisymmetric structure of the $\tilde{g}_{q,ij}^A$, see Eq. (2.4), there are no SUSY diagrams at the one-loop level. The LO result for the partonic process $gg \rightarrow A$ is thus determined solely by diagrams of the type shown in Fig. 1 (a). It reads explicitly [20–23]:

$$\begin{aligned} \hat{\sigma}_{gg}(x) &= \sigma_0^A \delta(1-x) + \mathcal{O}(\alpha_s^3), \\ \sigma_0^A &= \frac{\pi}{256v^2} \left(\frac{\alpha_s}{\pi} \right)^2 \left| \sum_{q \in \{t, b\}} \mathcal{A}_q(\tau_q) \right|^2, \\ \mathcal{A}_q(\tau_q) &= g_q^A \tau_q f(\tau_q), \quad \tau_q = \frac{4m_q^2}{M_A^2}, \end{aligned} \quad (2.7)$$

²The modifications for $p\bar{p}$ collisions are obvious and shall not be pointed out explicitly in this paper.

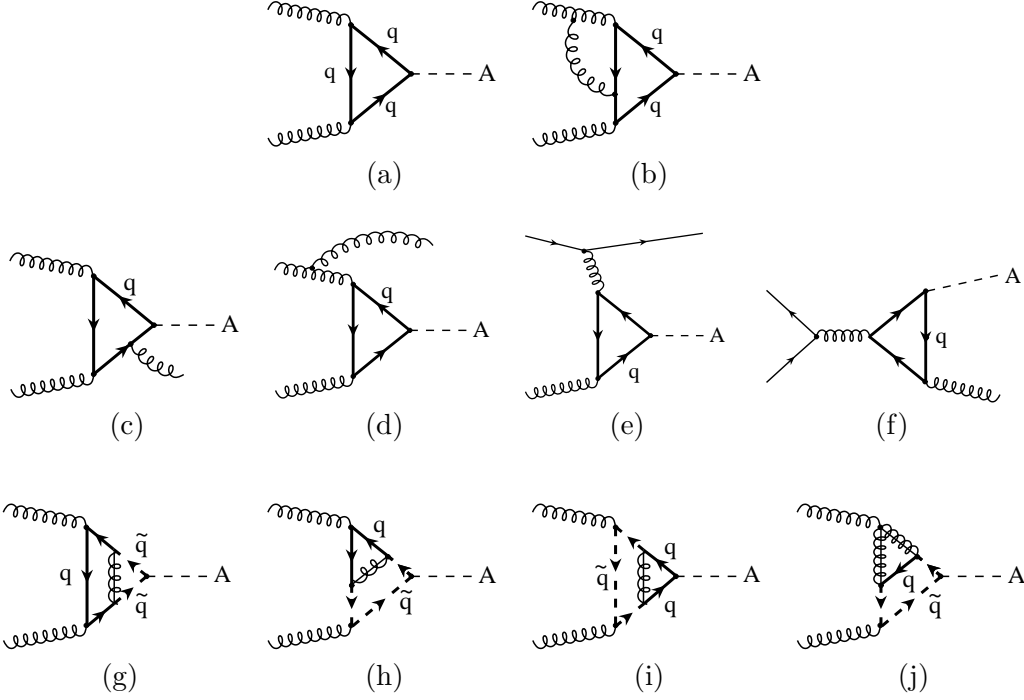


Figure 1: Diagrams contributing to the process $pp \rightarrow A + X$ in the MSSM at (a) LO and (b)–(j) NLO. According to the definition of the main text, (a)–(f) are referred to as “SM diagrams”, (g)–(j) as “SUSY diagrams”. The straight-curly line connecting quarks and squarks represents a gluino (denoted by \tilde{g} in the text).

where

$$f(\tau) = \begin{cases} \arcsin^2 \frac{1}{\sqrt{\tau}}, & \tau \geq 1, \\ -\frac{1}{4} \left[\ln \frac{1 + \sqrt{1 - \tau}}{1 - \sqrt{1 - \tau}} - i\pi \right]^2, & \tau < 1. \end{cases} \quad (2.8)$$

Throughout this paper, α_s denotes the strong coupling constant, renormalized in the $\overline{\text{MS}}$ scheme for QCD with five massless quark flavors.

3. Higher orders

3.1 Standard Model result – Effective Lagrangian

The SM contributions, based on \mathcal{L}_{SM} of Eq. (2.6), are known through NLO in terms of 1-dimensional integral representations [8,9], implemented in the program HIGLU [24]. They include both top and bottom quark loops as shown in Fig. 1 (a)–(f) ($q \in \{b, t\}$).

It has been shown in Ref. [9,10] that the NLO top quark contributions are well approximated by the formula

$$\sigma_t^{\text{NLO}} = K_\infty \sigma_t^{\text{LO}}, \quad \text{where} \quad K_\infty = \frac{\sigma_\infty^{\text{NLO}}}{\sigma_\infty^{\text{LO}}}. \quad (3.1)$$

σ_∞ is the cross section evaluated in an effective theory, obtained by integrating out the top quark:

$$\mathcal{L}_{\text{QCD}} + \mathcal{L}_{qA} \xrightarrow{mt \gg M_A} \mathcal{L}_{ggA}^{\text{SM}} = -\frac{A}{v} \left[\tilde{C}_1^{\text{SM}} \tilde{\mathcal{O}}_1 + \tilde{C}_2^{\text{SM}} \tilde{\mathcal{O}}_2 \right] + \mathcal{L}_{\text{QCD}}^{(5)}. \quad (3.2)$$

The operators are defined as

$$\tilde{\mathcal{O}}_1 = \frac{1}{4} \varepsilon^{\mu\nu\alpha\beta} G_{\mu\nu}^a G_{\alpha\beta}^a, \quad \tilde{\mathcal{O}}_2 = \sum_{q \neq t} \partial_\mu (\bar{q} \gamma^\mu \gamma_5 q). \quad (3.3)$$

Here, $\{q\} := \{d, u, s, c, b\}$ denotes the set of light (in our case massless) quark fields and $G_{\mu\nu}^a$ the gluon field strength tensor. $\mathcal{L}_{\text{QCD}}^{(5)}$ is the Standard QCD Lagrangian with five quark flavors.

The Wilson coefficients \tilde{C}_1^{SM} and \tilde{C}_2^{SM} have been calculated through NNLO in Ref. [16]. \tilde{C}_2^{SM} contributes only at NNLO and shall not be discussed any further in this paper. The result for \tilde{C}_1^{SM} is

$$\tilde{C}_1^{\text{SM}} = -\cot \beta \frac{\alpha_s}{16\pi} + \mathcal{O}(\alpha_s^4), \quad (3.4)$$

as it had been previously suggested in Refs. [8, 25, 26] on the basis of the Adler-Bardeen theorem [27].

$\tilde{\mathcal{O}}_1$ generates vertices which couple two and three gluons to the pseudo-scalar Higgs boson (the $gggA$ -vertex vanishes according to the Jacobi identity of the structure functions of SU(3)). Sample diagrams that contribute to the NLO cross section in the effective theory of Eq. (3.2) are shown in Fig. 2. The full set has been calculated through NLO in Ref. [8, 9], and through NNLO in Ref. [3, 4, 6].

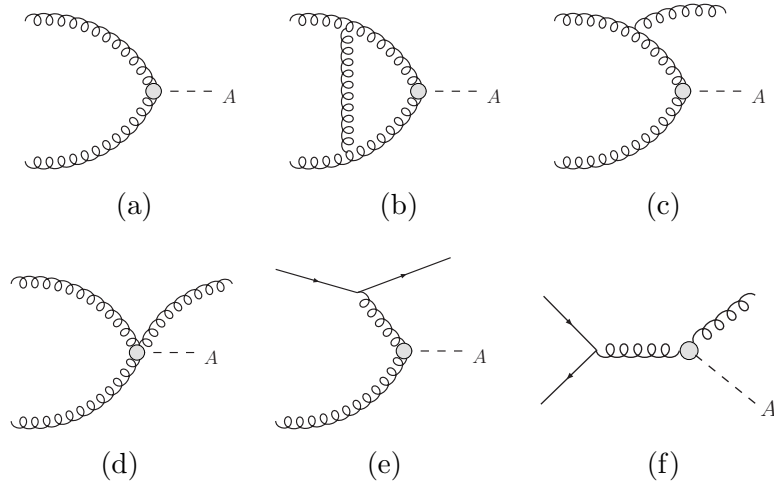


Figure 2: Diagrams contributing to the gluon fusion process in the effective theory at NLO.

3.2 SUSY contributions

We construct again an effective theory, this time by integrating out not only the top quark, but also all the SUSY particles. Since the remaining degrees of freedom are the same as in

the Standard Model case of Sect. 3.1, the effective Lagrangian has exactly the same form as in Eq. (3.2), only with \tilde{C}_1^{SM} and \tilde{C}_2^{SM} replaced by \tilde{C}_1 and \tilde{C}_2 .

As in the SM case, \tilde{C}_2 is zero through NLO. It remains to determine \tilde{C}_1 within the framework of Eq. (2.1) through NLO in α_s . The calculation of the SM case in Ref. [16] was done using Dimensional Regularization as it is most convenient for loop calculations in QCD. It is known that DREG breaks SUSY and requires SUSY-restoring finite counter terms in general. In the current case, however, these are not required due to the absence of SUSY contributions at LO.

On the other hand, one may apply Dimensional Reduction [28] in order to regularize the divergent integrals. This is done by setting $D = 4$ after contracting all (Lorentz and spinor) indices [29, 30], while the loop integrals are subsequently evaluated in $D = 4 - 2\epsilon$ dimensions.

A particularly subtle issue is the treatment of γ_5 which occurs in the Higgs–quark–anti-quark and the gluino–quark–squark vertex. We anticommute these γ_5 matrices and use $\gamma_5^2 = 1$ until only one of them remains in the Fermion trace. Working in DREG, we may follow the calculation of Ref. [16] which adopted the method of Ref. [14, 31, 32] for the treatment of γ_5 . This involves a finite counter term Z_5^p in order to restore gauge invariance [33]. Since there are no SUSY diagrams at LO, Z_5^p is given by the well-known SM expression quoted in Ref. [16].

For the DRED calculation, on the other hand, we simply set [14, 16, 32]

$$\gamma_5 = \frac{i}{4!} \varepsilon_{\mu\nu\rho\sigma} \gamma^\mu \gamma^\nu \gamma^\rho \gamma^\sigma. \quad (3.5)$$

It has been shown that the occurrence of the Levi-Civita symbol $\varepsilon_{\mu\nu\rho\sigma}$ can lead to inconsistencies when implemented in DRED [11]. We circumvent them by keeping the genuinely 4-dimensional Levi-Civita symbol $\varepsilon_{\mu\nu\rho\sigma}$ uncontracted until after the renormalization procedure, in close analogy to Refs. [16, 32]. As opposed to the calculation in DREG [16], however, working in DRED by definition does not involve terms of $\mathcal{O}(\epsilon = 2 - D/2)$ that require the above-mentioned finite counter terms in order to restore gauge invariance. We have verified that the scalar and pseudo-scalar one-loop quark vertices are identical in the chiral limit. Thus, the formulae of Ref. [16] for projecting onto the coefficient function \tilde{C}_1 can be translated to the DRED case by setting $D = 4$ and ignoring the finite renormalization of the pseudo-scalar current (i.e., $Z_5^p = 1$).

We will explicitly demonstrate that the SM result is recovered (through $\mathcal{O}(\alpha_s^3)$) by making all the superpartner masses infinitely heavy. It turns out that the SUSY diagrams lead to terms that do not vanish as $M_{\text{SUSY}} \rightarrow \infty$. However, they cancel with the counter terms of the SM diagrams to give the correct SM result.

The generalization of this approach for the implementation of γ_5 within DRED through higher orders is very desirable, of course, because it greatly simplifies precision calculations in SUSY models as they might be required by future experimental data.

4. Results

The evaluation of the diagrams proceeds in complete analogy to Ref. [7]. At NLO, one needs to evaluate massive 2-loop diagrams with vanishing external momenta. This is possible in a fully analytic way with the help of the algorithm of Ref. [34]³. As a cross check, we also calculated the diagrams in the limit $m_t \ll m_{\tilde{t}_1} \ll m_{\tilde{t}_2} \ll m_{\tilde{g}}$ by using automated asymptotic expansions [36] and found agreement with the corresponding expansion of the analytical result.

Subsequently, the bare coupling constant within the SUSY-QCD theory is transformed to its renormalized 5-flavor QCD expression in the $\overline{\text{MS}}$ scheme as described in Ref. [7].

In DRED, and using the prescription for the treatment of γ_5 described above, we find the following contribution of all SM diagrams to the coefficient function:

$$\tilde{C}_1|_{\text{SM-dias}} = -\frac{\alpha_s}{16\pi} \cot\beta \left\{ 1 - \frac{2}{3} \frac{\alpha_s}{\pi} \right\} + \mathcal{O}(\alpha_s^3). \quad (4.1)$$

The second term in the curly brackets arises from the MSSM expression for the quark mass counter term. Using the SM expression instead, we recover the well-known result of Eq. (3.4). The SUSY diagrams add up to

$$\tilde{C}_1|_{\text{SUSY-dias}} = -\frac{\alpha_s}{16\pi} \cot\beta \left\{ \frac{2}{3} \frac{\alpha_s}{\pi} \right\} + \mathcal{O}\left(\frac{m_t^2}{M^2}\right) + \mathcal{O}(\alpha_s^3), \quad M \in \{m_{\tilde{t}}, m_{\tilde{g}}\}, \quad (4.2)$$

such that indeed the SM limit is recovered as the SUSY masses are decoupled:

$$\tilde{C}_1^{\text{SM}} = \lim_{M_{\text{SUSY}} \rightarrow \infty} \left(\tilde{C}_1|_{\text{SM-dias}} + \tilde{C}_1|_{\text{SUSY-dias}} \right). \quad (4.3)$$

The general NLO result for \tilde{C}_1 can then be cast into the following form:

$$\tilde{C}_1 = -\frac{\alpha_s}{16\pi} \cot\beta \left\{ 1 + \frac{\alpha_s}{\pi} \frac{\mu_{\text{SUSY}}}{m_{\tilde{g}}} (\cot\beta + \tan\beta) f(m_t, m_{\tilde{t}_1}, m_{\tilde{t}_2}, m_{\tilde{g}}) \right\} + \mathcal{O}(\alpha_s^3). \quad (4.4)$$

A few observations may be worth pointing out:

- Eq. (4.4) immediately shows that the NLO corrections to the coefficient function will get more important w.r.t. the LO term for large values of $\tan\beta$ and μ_{SUSY} . On the other hand, large values of $\tan\beta$ increase the importance of bottom contributions even more, so that they usually obscure the squark effects.
- The $\mathcal{O}(\alpha_s^2)$ corrections are proportional to μ_{SUSY} , while the squark mixing angle θ_t (or, equivalently, the trilinear coupling A_t) drops out in the final result. This is due to the axial U(1) Peccei-Quinn symmetry of the SUSY potential [23,37] whose explicit breaking by the μ_{SUSY} term violates the Adler-Bardeen theorem. It provides another consistency check of our calculation.

³We are indebted to M. Steinhauser for providing us with his implementation of this algorithm in the framework of MATAD [35].

- As a result of the absence of mass terms at LO, the explicit form of f is independent of the mass renormalization scheme.
- Eqs. (4.1) and (4.2) are unchanged in DREG if the SM diagrams are multiplied by the finite renormalization constant Z_5^p (see Sect. 3.2 and Ref. [16]).

The general result for $f(m_t, m_{\tilde{t}_1}, m_{\tilde{t}_2}, m_{\tilde{g}})$ is too voluminous to be displayed here. Instead, we implemented \tilde{C}_1 in the program `evalcsusy.f` [7]⁴ and analyze its behavior numerically as shown in Sect. 5.

For practical purposes, it might be useful to provide the analytical expression of the function f for some limiting cases. Defining two mass scales $m \ll M$, and

$$x = \frac{m^2}{M^2}, \quad l_x = \ln(x), \quad (4.5)$$

we find

$$f(m, m, m, m) = \frac{5}{18} - \frac{9}{2} S_2 = -0.894176 \dots, \quad (4.6)$$

$$f(m, M, M, M) = -\frac{1}{3} - x \left(\frac{35}{54} - \frac{5}{36} l_x \right) - x^2 \left(\frac{41}{1800} + \frac{7}{60} l_x \right) + \dots, \quad (4.7)$$

$$f(m, m, m, M) = \frac{2}{3} + \frac{2}{3} l_x + x \left(\frac{7}{6} - \frac{1}{3} \zeta_2 + \frac{13}{6} l_x - \frac{1}{6} l_x^2 \right) + \dots, \quad (4.8)$$

$$f(M, m, m, m) = \frac{3}{2} + \frac{3}{2} l_x + x \left(\frac{11}{3} + 3 \zeta_2 + \frac{29}{3} l_x + \frac{3}{2} l_x^2 \right) + \dots, \quad (4.9)$$

$$f(m, M, M, m) = -\frac{13}{6} x - x^2 \left(\frac{22}{3} + 3 \zeta_2 + \frac{31}{3} l_x + \frac{3}{2} l_x^2 \right) + \dots, \quad (4.10)$$

$$f(m, m, M, M) = -\frac{2}{3} - x \left(\frac{181}{108} + \frac{13}{36} l_x \right) + \dots, \quad (4.11)$$

where the dots denote higher orders in x , and

$$S_2 = \frac{4}{9\sqrt{3}} \text{Cl}_2 \left(\frac{\pi}{3} \right), \quad \zeta_2 = \frac{\pi^2}{6}. \quad (4.12)$$

Insertion of $f(m, m, m, M)$ into Eq. (4.4) shows that, in contrast to scalar Higgs production [7, 38, 39], the result for \tilde{C}_1 is well-behaved as $m_{\tilde{g}} \rightarrow \infty$ at finite m . This is because there are no squark contributions at LO which could affect the renormalization of the NLO terms. The same holds for $m_{\tilde{t}} \rightarrow \infty$ as can be seen from the form of $f(m, M, M, m)$. Note, however, that the result is logarithmically divergent in the case where $m_t \rightarrow \infty$ with the other masses fixed, see $f(M, m, m, m)$. This is due to the linear mass dependence of the top Yukawa coupling and can be observed already in the pure SM contributions at higher orders in α_s .

⁴ The program is available from <http://www-ttp.physik.uni-karlsruhe.de/Progdata/ttp04/ttp04-19>.

5. Discussion

5.1 Coefficient function \tilde{C}_1

We will now discuss the numerical effect of the newly evaluated terms. First, we investigate the dependence of \tilde{C}_1 on the squark and gluino masses. To this aim, it is convenient to consider the leading and the NLO term separately:

$$\tilde{C}_1 = -\frac{\alpha_s}{16\pi} \left(\tilde{c}_1^{(0)} + \frac{\alpha_s}{\pi} \tilde{c}_1^{(1)} \right) + \mathcal{O}(\alpha_s^3). \quad (5.1)$$

According to Eq. (4.4),

$$\tilde{c}_1^{(0)} = \cot \beta. \quad (5.2)$$

Fig. 3 shows $\tilde{c}_1^{(1)}$ as a function of $m_{\tilde{g}}$ for various values of $m_{\tilde{t}_1}$ and $m_{\tilde{t}_2}$. In Fig. 4, on the other hand, we consider it as a function of one of the stop masses ($m_{\tilde{t}_A}$) while fixing $m_{\tilde{g}}$ and the other stop mass ($m_{\tilde{t}_B}$) at a few representative values; A and B assume the values 1 and 2, depending on whether $m_{\tilde{t}_A}$ is larger or smaller than $m_{\tilde{t}_B}$. Note that $\tilde{c}_1^{(1)}$ is symmetric in $m_{\tilde{t}_1}$ and $m_{\tilde{t}_2}$ since it does not depend on the squark mixing angle θ_t as mentioned above. Finally, in Fig. 5, $m_{\tilde{t}_1} = m_{\tilde{t}_2} = m_{\tilde{t}}$ is varied for certain choices of $m_{\tilde{g}}$.

The general structure is quite similar in all figures: $\tilde{c}_1^{(1)}$ is of the order of -0.5 for moderate values of the SUSY masses. As they increase, $\tilde{c}_1^{(1)}$ tends to zero in agreement with the general discussion above. In order to demonstrate this behavior more clearly, Fig. 6 adopts the same parameters as Fig. 3, but extends up to very large values of the gluino mass.

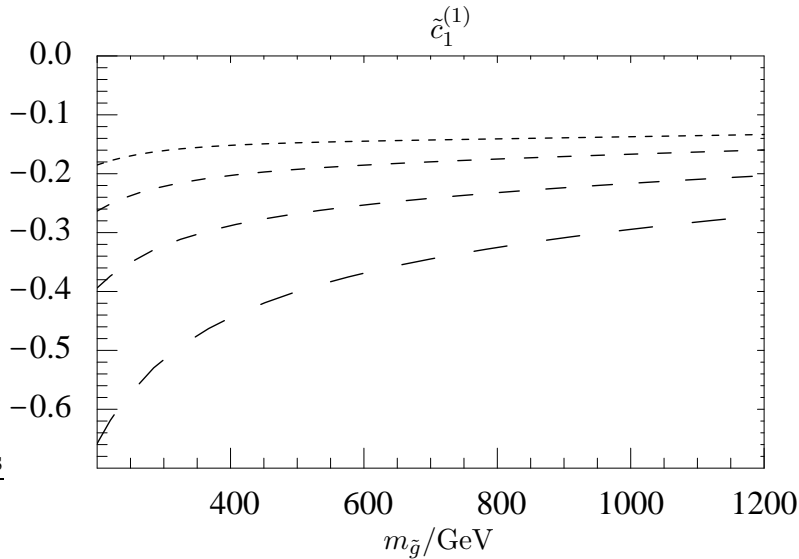


Figure 3: $\tilde{c}_1^{(1)}$ as a function of the gluino mass for $m_t = 173$ GeV, $\mu_{\text{SUSY}} = 150$ GeV, $\tan \beta = 3$, and $(m_{\tilde{t}_1}, m_{\tilde{t}_2}) = (200, 200)/(200, 400)/(200, 600)/(400, 600)$ GeV [long/.../short dashes].

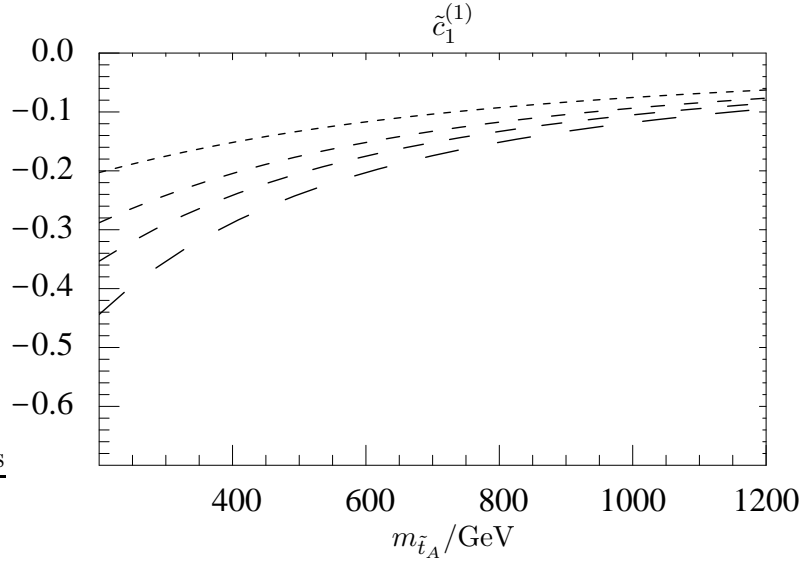


Figure 4: $\tilde{c}_1^{(1)}$ as a function of $m_{\tilde{t}_A}$ for $m_t = 173$ GeV, $\mu_{\text{SUSY}} = 150$ GeV, $\tan \beta = 3$, $m_{\tilde{g}} = 400$ GeV, and $m_{\tilde{t}_B} = 200/300/400/600$ GeV [long/.../short dashes]; $[(A, B) = (1, 2)$ if $m_{\tilde{t}_A} \leq m_{\tilde{t}_B}$, otherwise $(A, B) = (2, 1)$].

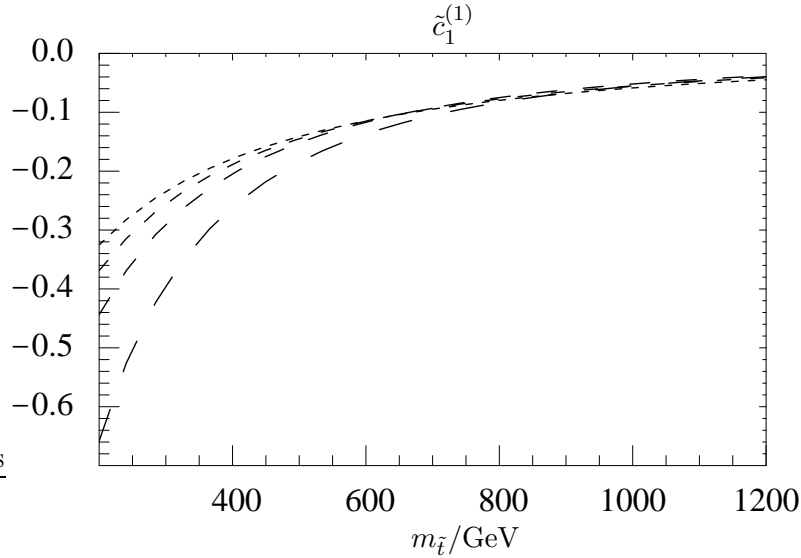


Figure 5: $\tilde{c}_1^{(1)}$ as a function of $m_{\tilde{t}} \equiv m_{\tilde{t}_1} = m_{\tilde{t}_2}$ for $m_t = 173$ GeV, $\mu_{\text{SUSY}} = 150$ GeV, $\tan \beta = 3$, $m_{\tilde{g}} = 200/400/600/800$ GeV [long/.../short dashes].

For the discussion of the numerical effects on the cross section in the following section, we adopt a scenario similar to the m_h^{max} benchmark scenario [40], corresponding to

$$m_{\tilde{t}_1} = 826 \text{ GeV}, \quad m_{\tilde{t}_2} = 1172 \text{ GeV}, \quad m_{\tilde{g}} = 800 \text{ GeV}. \quad (5.3)$$

In the original definition of this scenario, μ_{SUSY} was set to -200 GeV; here, however, we will allow for a variation of this parameter between ± 1 TeV. In addition, we will assume

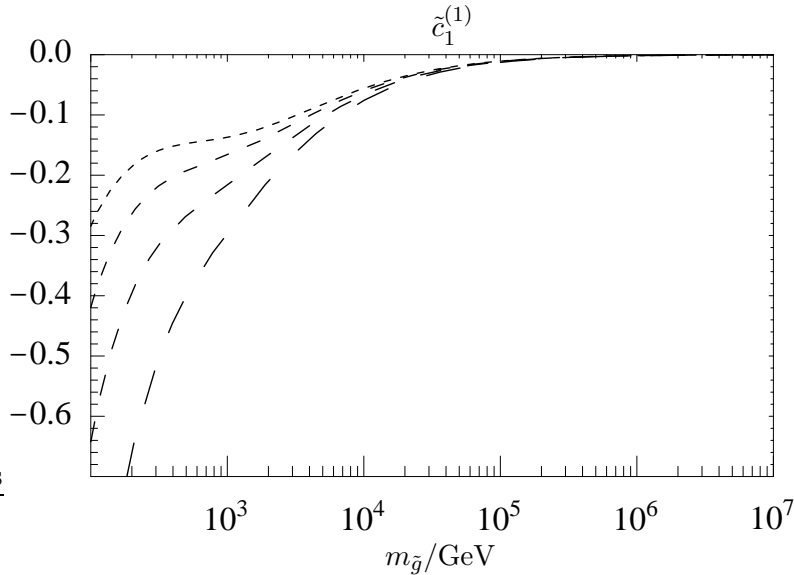


Figure 6: Same as Fig. 3, but extended abscissa in order to demonstrate the asymptotic behavior of $\tilde{c}_1^{(1)}$.

$\tan \beta = 3$; the top mass is set to $m_t = 173 \text{ GeV}$.⁵

The 2-loop term of the coefficient function is then given by

$$\tilde{c}_1^{(1)} = -0.392 \frac{\mu_{\text{SUSY}}}{1 \text{ TeV}}. \quad (5.4)$$

5.2 Effects on the cross section

The inclusive NLO hadronic cross section for pseudo-scalar Higgs production receives contributions from the subprocesses $gg \rightarrow A(+g)$, $qg \rightarrow Aq$, and $q\bar{q} \rightarrow Ag$. At this order, squarks only affect the process $gg \rightarrow A$, because of the antisymmetric structure of the $\tilde{q}_i \tilde{q}_j A$ coupling, cf. Eqs. (2.2), (2.4). Recalling the notation of Eq. (2.5), we write

$$\hat{\sigma}_{gg}(x) = \hat{\sigma}_{tb}(x) + \Delta \hat{\sigma}_{\tilde{t}t}(x) + \Delta \hat{\sigma}_{\tilde{t}b}(x) + \mathcal{O}(\alpha_s^4), \quad (5.5)$$

where $\hat{\sigma}_{tb}$ denotes the contributions arising from the top and bottom mediated gluon-Higgs couplings. It can be evaluated through NLO for arbitrary top, bottom, and Higgs masses with the help of the FORTRAN program HIGLU. The same is true for the qg and the $q\bar{q}$ sub-processes (see Figs. 1 (e) and (f)).

$\Delta \hat{\sigma}_{\tilde{t}t}$ and $\Delta \hat{\sigma}_{\tilde{t}b}$ are the effects arising from the interference of stop-induced with top- and bottom-induced amplitudes:

$$\Delta \hat{\sigma}_{\tilde{t}q} \sim \text{Re} \left(\mathcal{M}_{\tilde{t}}^{(1)*} \mathcal{M}_q^{(0)} \right), \quad q \in \{b, t\}. \quad (5.6)$$

⁵We remark that, for $M_A \lesssim 200 \text{ GeV}$, this choice of parameters leads to a conflict between the theoretical value of the light Higgs mass m_h (evaluated with `FeynHiggs` [41], for example) and its current experimental lower limit; nevertheless, for the sake of generality, we will vary M_A between 100 and 300 GeV in our numerical analyses below.

$\mathcal{M}_q^{(0)}$ is expressed in terms of \mathcal{A}_q from Eq. (2.7), while for $\mathcal{M}_{\tilde{t}}^{(1)}$, we use the expression evaluated in the effective theory to obtain

$$\Delta\hat{\sigma}_{\tilde{t}q}(x) = \frac{\pi}{128v^2} \left(\frac{\alpha_s}{\pi}\right)^3 \text{Re}\left(\hat{c}_1^{(1)} \mathcal{A}_q(\tau_q)\right) \delta(1-x). \quad (5.7)$$

Note that $\mathcal{M}_{\tilde{t}}^{(1)}$ has a branch cut at $M_A = 2m_t$. Thus, we expect our result to be valid for $M_A < 2m_t$. Recall, however, that in the SM case, the heavy top limit still provides an excellent approximation for Higgs masses much larger than $2m_t$ [9, 10, 42, 43].

To study the numerical effects, we consider the modified m_h^{max} scenario quoted in Eq. (5.3). Fig. 7 shows the relative size of the top squark effects to the total NLO cross section. We note that even for $|\mu_{\text{SUSY}}| = 1 \text{ TeV}$, they hardly exceed 4%.

Fig. 8 shows separately the effects of the top-stop and the bottom-stop interference terms, again relative to the total NLO cross section, for $\mu = 1 \text{ TeV}$. They are of similar order in magnitude, but opposite in sign, thus cancelling each other to a certain extent.

Finally, Fig. 9 shows the inclusive cross section through NLO for the modified m_h^{max} scenario defined in and below Eq. (5.3), including effects of top and bottom quarks (solid line) as well as top squarks (dashed lines) for $\mu_{\text{SUSY}} = \pm 1 \text{ TeV}$.

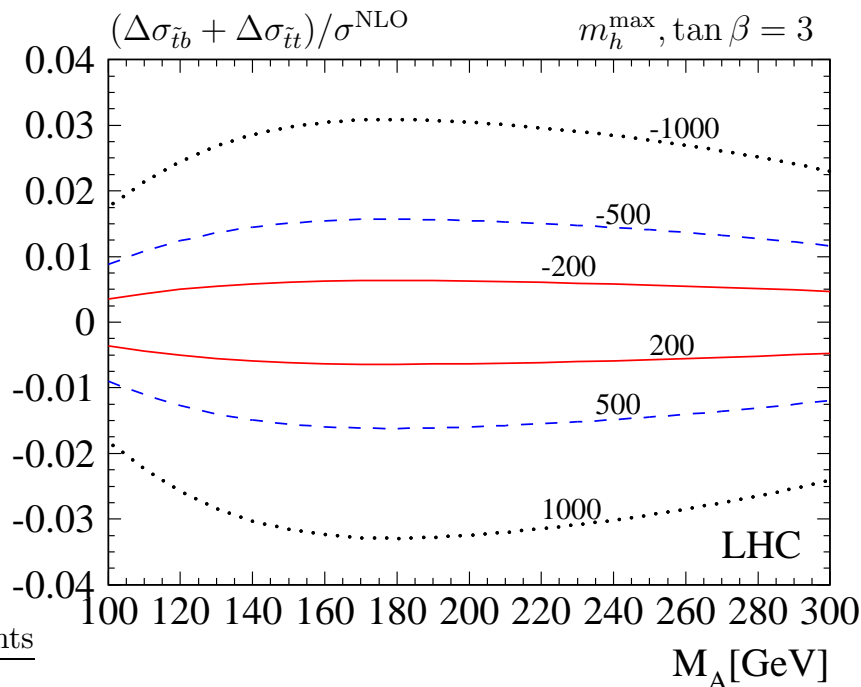


Figure 7: Effects of the top-stop and bottom-stop interference terms relative to the total NLO cross section for the scenario defined in and below Eq. (5.3). The numbers above the graphs denote the value of μ_{SUSY} in GeV.

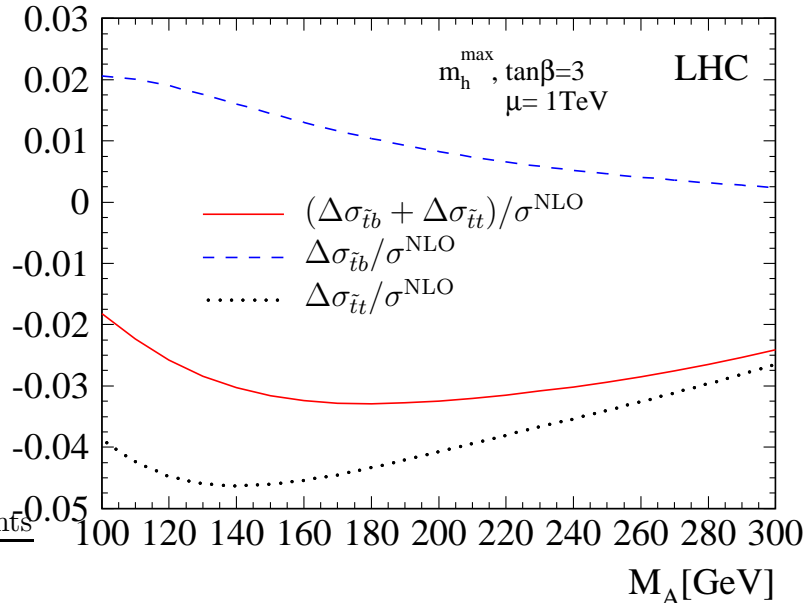


Figure 8: Relative effect of the top-stop (dotted) and bottom-stop (dashed) interference terms, as well as their sum (solid), for the scenario defined in and below Eq. (5.3).

6. Conclusions

The corrections to the effective Higgs-gluon coupling for a pseudo-scalar Higgs boson have been evaluated in the MSSM through first order in the strong coupling constant α_s , taking into account effects of top and bottom quarks as well as top squarks. The NLO corrections are proportional to μ_{SUSY} as expected from the symmetries of the SUSY potential. The numerical effects were studied within a specific SUSY scenario, derived from the m_h^{\max} scenario of Ref. [40]; further studies can be performed easily using the publicly available numerical routine `evalcsusy.f` (see footnote on page 9).

The calculation also addresses a technical issue, since it involves the γ_5 matrix in a non-trivial way. In analogy to Ref. [16], we avoided the contraction of the Levi-Civita symbol with D dimensional quantities. We argued that the calculation in DRED does not require finite counter terms as opposed to the DREG approach, provided the underlying theory is supersymmetric. The result was confirmed by evaluating the diagrams in DREG and including the proper counter term for γ_5 .

It would be interesting to investigate these observations in more detail, in particular to prove the validity of our implementation of γ_5 within DRED in a rigorous way. Further corroboration could be obtained from its application at second order α_s . This corresponds to the evaluation of \tilde{C}_1 at three loops for which the technical tools are in principle available [44].

From the phenomenological point of view, inclusion not only of bottom but also sbottom

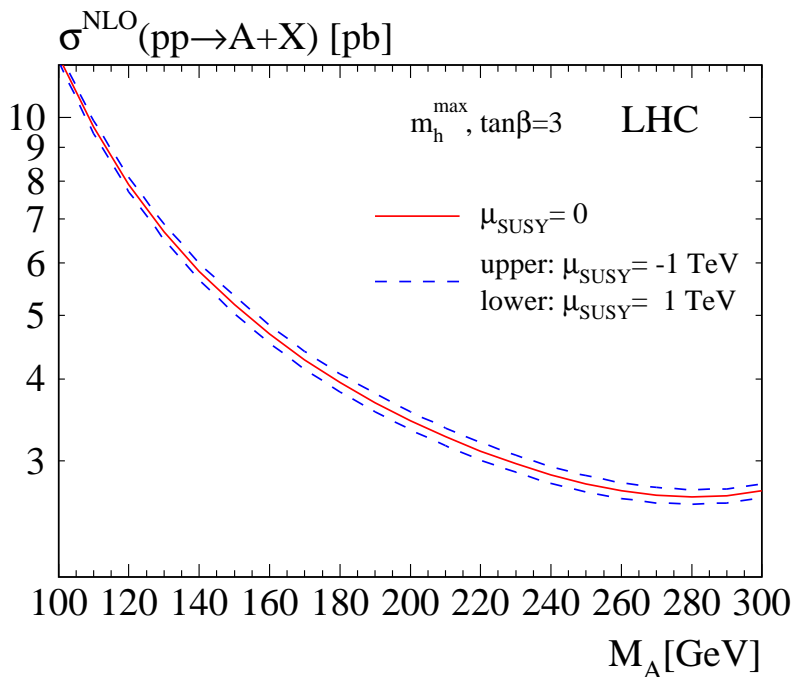


Figure 9: Total cross section at NLO including top and bottom effects (solid). Stop effects (dashed) are shown for the scenario defined in and below Eq. (5.3) for two choices of μ_{SUSY} .

quarks would be desirable. This could be done in the heavy sbottom limit using asymptotic expansions of Feynman diagrams. Moreover, one could calculate the photonic decay rate of the CP-odd Higgs boson in a very similar fashion. There, however, one does not need to rely strictly on the effective Lagrangian, but could evaluate the first few terms of a Taylor expansion in M_{A}^2/M^2 along the lines of Ref. [45], where $M \in \{m_t, m_{\tilde{t}}, m_{\tilde{g}}\}$.

Acknowledgments. We are grateful to K. Chetyrkin for various helpful comments and advice. We would like to thank S. Heinemeyer for his advice on SUSY benchmark scenarios, M. Steinhauser for enlightening discussions concerning the treatment of γ_5 , and D. Stöckinger for his constructive comments on the manuscript. We are particularly indebted to J. Reuter for his help in interpreting the structure of Eq. (4.4), and to M. Spira for clarifications concerning the DREG approach in this calculation, and various suggestions for improvement. Further thanks go to A. Djouadi and J. Kühn for encouragement and inspiring conversations.

We kindly acknowledge financial support by *Deutsche Forschungsgemeinschaft* (contract HA 2990/2-1, *Emmy Noether program*).

References

- [1] A. Djouadi, [arXiv:hep-ph/0503172](https://arxiv.org/abs/hep-ph/0503172); [arXiv:hep-ph/0503173](https://arxiv.org/abs/hep-ph/0503173).

- [2] R.V. Harlander and W.B. Kilgore, *Phys. Rev. Lett.* **88**, 201801 (2002).
- [3] R.V. Harlander and W.B. Kilgore, *JHEP* **0210**, 017 (2002).
- [4] C. Anastasiou and K. Melnikov, *Phys. Rev. D* **67**, 037501 (2003).
- [5] C. Anastasiou and K. Melnikov, *Nucl. Phys. B* **646**, 220 (2002).
- [6] V. Ravindran, J. Smith, W.L. van Neerven, *Nucl. Phys. B* **665**, 325 (2003).
- [7] R.V. Harlander and M. Steinhauser, *JHEP* **0409**, 066 (2004).
- [8] M. Spira, A. Djouadi, D. Graudenz, P.M. Zerwas, *Phys. Lett. B* **318**, 347 (1993).
- [9] M. Spira, A. Djouadi, D. Graudenz, P.M. Zerwas, *Nucl. Phys. B* **453**, 17 (1995).
- [10] M. Spira, *Fortschr. Phys.* **46**, 203 (1998).
- [11] W. Siegel, *Phys. Lett. B* **94**, 37 (1980).
- [12] J. Smith and W.L. van Neerven, *Eur. Phys. J. C* **40**, 199 (2005).
- [13] D. Stöckinger, *JHEP* **0503**, 076 (2005).
- [14] G. 't Hooft and M.J. Veltman, *Nucl. Phys. B* **44**, 189 (1972).
- [15] P. Breitenlohner and D. Maison, *Comp. Phys. Commun.* **52**, 11 (1977).
- [16] K.G. Chetyrkin, B.A. Kniehl, M. Steinhauser, W.A. Bardeen, *Nucl. Phys. B* **535**, 3 (1998).
- [17] S. Kraml, PhD thesis, Vienna University (1999), [arXiv:hep-ph/9903257](#).
H. Eberl, PhD thesis, Vienna University (1998).
- [18] A.D. Martin, R.G. Roberts, W.J. Stirling, R.S. Thorne, *Eur. Phys. J. C* **23**, 73 (2002).
- [19] A.D. Martin, R.G. Roberts, W.J. Stirling, R. S. Thorne, *Eur. Phys. J. C* **35**, 325 (2004).
- [20] P. Kalyniak, R. Bates, J.N. Ng, *Phys. Rev. D* **33**, 1986 (755).
- [21] R. Bates, J.N. Ng, P. Kalyniak, *Phys. Rev. D* **34**, 1986 (172).
- [22] J.F. Gunion, G. Gamberini, S.F. Novaes, *Phys. Rev. D* **38**, 1988 (3481).
- [23] J.F. Gunion, H.E. Haber, G. Kane, S. Dawson, *The Higgs Hunter's Guide*, Addison-Wesley, 1990.
- [24] M. Spira, [arXiv:hep-ph/9510347](#).
- [25] R.P. Kauffman and W. Schaffer, *Phys. Rev. D* **49**, 551 (1994).
- [26] A. Djouadi, M. Spira, P.M. Zerwas, *Phys. Lett. B* **311**, 1993 (255).
- [27] S.L. Adler and W.A. Bardeen, *Phys. Rev.* **182**, 1517 (1969).
- [28] W. Siegel, *Phys. Lett. B* **84**, 193 (1979).
- [29] I. Jack, D.R.T. Jones, K.L. Roberts, *Z. Phys. C* **63**, 151 (1994).
- [30] I. Jack and D.R.T. Jones, [arXiv:hep-ph/9707278](#).
- [31] D.A. Akyeampong and R. Delbourgo, *Nuovo Cim.* **17A**, 578 (1973).
- [32] S.A. Larin, *Phys. Lett. B* **303**, 113 (1993).
- [33] T.L. Trueman, *Phys. Lett. B* **88**, 331 (1979).

- [34] A.I. Davydychev and J.B. Tausk, *Nucl. Phys.* **B 397**, 123 (1993).
- [35] M. Steinhauser, *Comp. Phys. Commun.* **134**, 335 (2001).
- [36] T. Seidensticker, [arXiv:hep-ph/9905298](#).
R. Harlander, T. Seidensticker, M. Steinhauser, *Phys. Lett.* **B 426**, 125 (1998).
- [37] J. Reuter, private communication.
- [38] R.V. Harlander and M. Steinhauser, *Phys. Lett.* **B 574**, 258-268 (2003).
- [39] R.V. Harlander and M. Steinhauser, *Phys. Rev.* **D 68**, 111701 (2003).
- [40] M. Carena, S. Heinemeyer, C.E.M. Wagner, G. Weiglein, [arXiv:hep-ph/9912223](#).
- [41] S. Heinemeyer, W. Hollik, G. Weiglein, *Comp. Phys. Commun.* **124**, 2000 (76).
- [42] M. Krämer, E. Laenen, M. Spira, *Nucl. Phys.* **B 511**, 523 (1998).
- [43] R. Harlander, [arXiv:hep-ph/0311005](#).
- [44] R. Harlander and M. Steinhauser, *Prog. Part. Nucl. Phys.* **43**, 167 (1999).
- [45] M. Steinhauser, [arXiv:hep-ph/9612395](#).